Chapter 1
Solid Solution

1.1 Solubility

Hydrogen that brings about degradation of metallic materials comes from environments. Hydrogen adsorbs on the surface of metal in the form of H_2 molecule or H_3O^+ ion, dissociates to atoms, and diffuses into the bulk. Hydrogen atoms locate at various sites in metals with respective energies at sites as schematically shown in Fig. 1.1. The role of hydrogen in embrittlement is the central subject in this book, and interactions of hydrogen with various lattice defects are of crucial importance. Hydrogen atoms in solid solution, i.e., at interstitial sites of the regular lattice, are only a part of the total hydrogen atoms in most cases at thermal equilibrium, but interstitial sites are dominating in the number and control the transport and partition of hydrogen at various trap sites.

The temperature dependence of the solid solubility θ of hydrogen in various metals in hydrogen gas of 0.1 MPa are compared in Fig. 1.2 [1]. The negative slope in the Arrhenius plot for iron means an endothermic reaction for hydrogen absorption, i.e., the energy of hydrogen in solid solution is higher than that in hydrogen molecule as Fig. 1.1 indicates. It is in contrast with Ti and V that have higher affinities with hydrogen than Fe. The amount of absorbed hydrogen in iron at high temperatures is readily measured by chemical analysis. Thus, determined solid solubility data for pure iron under hydrogen gas environments above 300 °C are shown in Fig. 1.3 [2]. The ordinate denotes $\boldsymbol{\theta}$ in atomic ratio normalized by $\sqrt{p}$, where p is the hydrogen gas pressure in the unit of 0.1 MPa. Solubility data at lower temperatures are shown in Sect. 2.1 concerning trapping of hydrogen in lattice defects.

In Fig. 1.3, the level of $\boldsymbol{\theta}$ in face-centered cubic (fcc) $\boldsymbol{\gamma}$-iron is higher than that in body-centered cubic (bcc) $\boldsymbol{\alpha}$-iron, and a slight departure from the Arrhenius plot appears at temperatures lower than about 500 °C. The departure was discussed to originate in simultaneous occupations of tetrahedral and octahedral sites in α-iron [2]. Definitive values of $\boldsymbol{\theta}$ in $\boldsymbol{\alpha}$-iron in the room temperature regime are few, and

M. Nagumo, *Fundamentals of Hydrogen Embrittlement*,
DOI 10.1007/978-981-10-0161-1_1

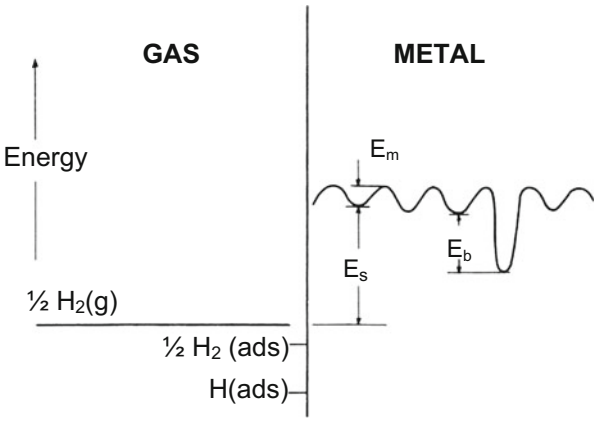

Fig. 1.1 Energies of hydrogen in gas-metal equilibria. E_s, energy of solid solution; E_m, migration energy; E_b, trap binding energy

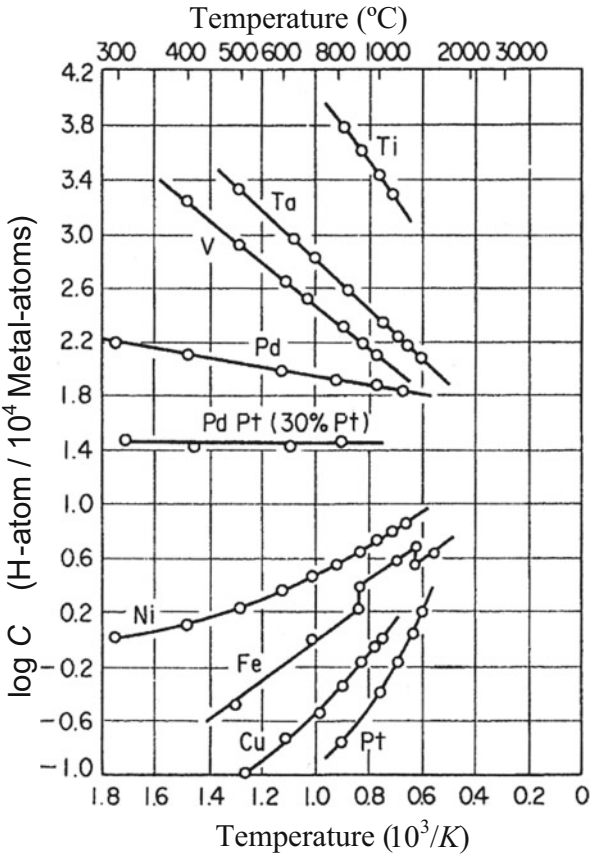

Fig. 1.2 Temperature dependence of hydrogen solubility in various metals in equilibrium at 0.1 MPa hydrogen gas (Huang et al. [1]. Reprinted with permission from The Japan Inst. Metals)

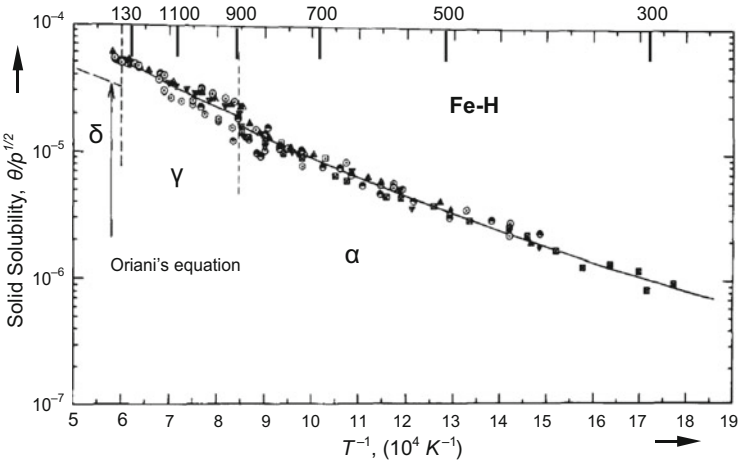

Fig. 1.3 Solid solubility of hydrogen in iron above 300 °C (Different marks are by literatures in the original paper. Da Silva et al. [2])

Hirth collected reliable data and expressed θ (in atomic ratio) in hydrogen gas of pressure p (in 0.1 MPa) in the form

$$\theta = 0.00185\sqrt{p}\,\exp\left(-3440/T\right) \tag{1.1}$$

with T in Kelvin [3]. The heat of solution of hydrogen in α-iron obtained from the temperature dependence of θ is 28.6 kJ/mol-H.

The $\sqrt{p}$ dependence of θ is known as Sieverts' law. It is originally an experimental relation for diatomic molecular gases, but it is also derived from thermodynamics. The entry of hydrogen into metal is initiated by the dissociation of adsorbed hydrogen molecules on the metal surface followed by the diffusion of hydrogen atoms into the metal. For the equilibrium reaction,

$$\frac{1}{2}H_2 \rightleftarrows H_{\mathrm{sol}}\,, \tag{1.2}$$

where the chemical potential μ is equal in both sides, i.e.,

$$\frac{1}{2}\mu_{H_2} = \mu_{H_{\mathrm{sol}}}. \tag{1.3}$$

Expressing μ in terms of the value at the standard state, μ^0, and the activity of hydrogen, a, in the form of

$$\mu = \mu^0 + RT \ln a, \tag{1.4}$$

where R is the gas constant, the change of the Gibbs energy associated with the absorption is written as

$$-\Delta G^0 = \frac{1}{2}\mu^0_{H_2} - \mu^0_{H_{sol}} = RT \ln \frac{a_{H_{sol}}}{a^{1/2}_{H_2}}. \tag{1.5}$$

Since

$$\Delta G^0 = \Delta H^0 - T\Delta S^0, \tag{1.6}$$

where H and S denote respectively enthalpy and entropy, Eq. (1.5) is rewritten as

$$a_{H_{sol}} = a^{1/2}_{H_2} \exp\left(-\frac{\Delta H^0}{RT}\right) \exp\left(\frac{\Delta S^0}{R}\right) \tag{1.7}$$

leading to the form of Sieverts' law.

It is to be noticed that the hydrogen concentration is expressed in terms of activity a and thus is related to pressure in terms of fugacity f:

$$a = \frac{f}{f^0} = \frac{\varphi p}{\varphi^0 p^0}, \tag{1.8}$$

where φ is the fugacity coefficient and the superscript "^{0}" denotes the standard state. Accordingly, for the estimation of the equilibrium hydrogen concentration using Eq. (1.1), p should be replaced by f. The conversion is important in practice for high pressures, since φ increases with p. Calculated values of φ are tabulated in Ref. [4], e.g., 1.06, 1.41 and 2.06 for p of 10, 50 and 100 MPa hydrogen gas at 300 K, but the values vary according to the equation of state employed for the calculation.

The equilibrium hydrogen concentration in α-iron at room temperature expected from Eq. (1.1) is very small, *ca* 2×10^{-8} (in atomic ratio), in 0.1 MPa hydrogen gas. Then, normally observed hydrogen concentrations of the order of mass ppm in ferritic steels are mostly the amount of trapped hydrogen in various lattice defects except under nonequilibrium situations.

The solubility of hydrogen in steels is substantially altered by alloying. In austenitic stainless steels, the heat of solution of hydrogen is about 16 kJ/mol-H [5], much less than that in pure γ-iron. Solubility data for stainless steels are shown in Fig. 1.4 [5]. Higher solubilities in austenitic stainless steels than those in ferritic stainless steels are due not only to the crystal structures but also to alloying elements such as Ni and Cr. Most data in Fig. 1.4 were obtained by permeation experiments. It is to be noticed that very inhomogeneous distributions of hydrogen are often present in austenitic stainless steels because of the low diffusivity of hydrogen as described in Sect. 4.1. At elevated temperatures, the increased

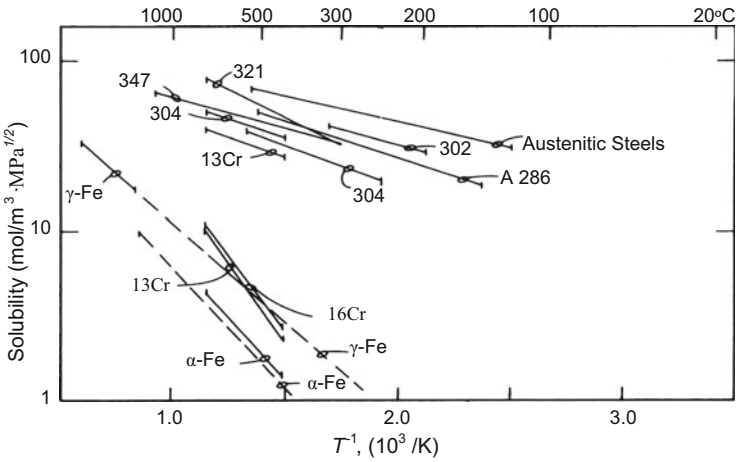

Fig. 1.4 Solid solubility data of hydrogen in stainless steels (Caskey [5])

diffusivity favors homogeneous distribution and the hydrogen content in Type 316 L stainless steel measured directly by means of thermal desorption is about 40 mass ppm in 70 MPa hydrogen at 90 °C [6].

1.2 Lattice Location

Hydrogen atoms locate at interstitial sites in the elementary lattice of α-iron. Direct determination of the location is difficult because of the small solubility and the high diffusivity of hydrogen, but the preferential occupancy at the tetragonal site (T-site) than at the octahedral site (O-site) has been shown by calculations of the total energy of the solution described in Sect. 1.4. Analyses of thermodynamic data also show that the T-site occupancy is favored at low temperatures, but the O-site occupancy increases as the temperature increases [2, 7].

A powerful method to detect directly the lattice location of hydrogen in metals is a channeling analysis utilizing a nuclear reaction $^{1}H(^{11}B,\alpha)\,\alpha\alpha$ using ^{11}B beam. The location of hydrogen can be precisely determined by measuring the angular profile of emitted α particles on tilting a single crystal specimen against the incident ^{11}B beam. Hydrogen occupancy at the T-site was successfully confirmed for bcc single crystals of the group V_a metals (Nb, V, Ta) and their alloys [8–11]. In vanadium, a reversible displacement of hydrogen from the normal T-site was observed when a compressive stress of 70 MPa was applied along the $<100>$ axis [8]. In Nb-Mo alloys with Mo of less than 10 %, the position of hydrogen atom shifts from the center of the T-site to a neighboring Mo atom as shown schematically in Fig. 1.5 [10]. The shift decreases with increasing Mo concentrations and disappears at 20 at % of Mo, showing a direct evidence for hydrogen trapping by alloying elements.

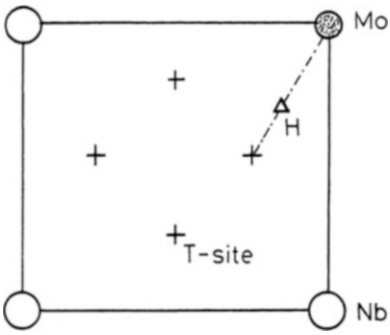

Fig. 1.5 Location of hydrogen atom in Nb-Mo alloy determined by a ^{1}H ($^{11}B\alpha)\alpha\alpha$ nuclear reaction channeling method (Yagi [10]. Reprinted with permission from The Iron & Steel Inst. Japan)

1.3 Partial Molar Volume and Strain Field

The entry of hydrogen into metals accompanies volume expansion, and the partial molar volume of hydrogen, $\overline{V}_H$, is directly obtained from dilatation measurements. While a substantial scatter of data is inevitable, a reliable value of $\overline{V}_H$ for α-iron wires exposed in hydrogen gas is 2.0×10^{-6} m^3/mol-H at the temperature range from 600 °C to 800 °C [12]. At room temperature, electrochemical hydrogen permeation experiments have been used to determine the value of $\overline{V}_H$. The steady-state permeation current in iron is affected by the applied elastic stress, and this effect is ascribed to the change of the hydrogen solubility. The chemical potential of hydrogen in metal is altered by applied stress, and an additional flow of hydrogen takes place to keep equilibrium. The hydrogen concentration is evaluated from the permeation current density, and $\overline{V}_H$ is given as [13],

$$\overline{V}_H = RT\left[\frac{\partial \ln (C_\sigma / C_0)}{\partial \sigma_h}\right], \tag{1.9}$$

where C_σ and C_0 are respectively hydrogen concentrations with and without the application of external hydrostatic stress σ_h. The values of C_σ and C_0 are estimated from reversible permeation current densities on cyclic stressing. The values of $\overline{V}_H$ thus calculated for pure iron and AISI 4340 steel are 2.66 and 1.96×10^{-6} m^3/mol-H, respectively [13], which are close to the value obtained from dilatation measurements at high temperatures. The value of $\overline{V}_H$ is insensitive to temperature and microstructures. The value of 2.0×10^{-6} m^3/mol-H, i.e., about 0.3 nm^3/H-atom, is almost common for all metals [7]. However, Hirth noticed [3] that the internal volume change δv due to lattice hydrogen to be used for calculating interactions with elastic fields was 1.22×10^{-6} m^3/mol-H when elastic relaxations at the free surface were taken into account for evaluating $\overline{V}_H$.

The volume change around hydrogen atom plays a crucial role in interaction energies of hydrogen with various types of lattice defects. In α-iron, the local strain field around a single hydrogen interstitial atom has tetragonal symmetry in both the *T*- and *O*-sites [3], but the tetragonality is considered to be small. Accordingly, in

the elastic regime, the hydrogen concentration, C_h, under hydrostatic stress σ_h, or C_σ under a uniaxial stress σ, at a constant hydrogen fugacity f is given respectively as

$$C_h = C_0 \exp\left(\frac{\sigma_h \overline{V}_H}{RT}\right)_f , \tag{1.10}$$

or

$$C_\sigma = C_0 \exp\left(\frac{\sigma \overline{V}_H}{3RT}\right)_f , \tag{1.11}$$

where C_0 is the value at zero stress [14].

Accumulation of hydrogen in stress-concentrated areas such as notch root has been revealed in steels by means of hydrogen microprint technique [15]. It should be noticed, however, that the increase in the hydrogen concentration by stress also results from trapping of hydrogen in various lattice defects created by plastic strain.

1.4 Atomistic Calculations of the Heat of Solution

In the crystalline lattice of metals, the electronic state of hydrogen differs from that of free atom because of partial sharing of electrons with host metallic ions. The heat of solution, H_s, is the difference between the energy of hydrogen atom in solid solution and a half of the energy of hydrogen molecule as shown in Fig. 1.1. Atomistic calculations of binding energies of hydrogen with metals have been conducted by various methods. The first-principles calculations are generally time consuming, and some approximate methods have been devised.

The effective medium theory (EMT) replaces the complicated inhomogeneous host by an effective host consisting of a homogeneous electron gas. The embedding energy ΔE of an atom is defined as the energy difference between the combined atom-host system minus the energies of the separated atom and the host. The host density is not homogeneous in general, and the core regions of host atoms have very large variations in the electrostatic potential. Nørskov took into account the interaction of the hydrogen 1 *s* level with the valence bands, particularly 3*d* band, of the host and calculated ΔE of hydrogen at the *T*-site of α-iron in transition metals [16]. Thus, calculated value of ΔE for α-iron was -212 kJ/mol. The heat of solution is the embedding energy minus the binding energy of hydrogen molecule (-232 kJ/mol), and the resultant 20 kJ/mol is close to experimentally obtained 29 kJ/mol [3, 17].

A generalization of the EMT using a pair-wise interaction is the embedded atom method (EAM) [18, 19]. It considers each atom in a system as embedded in a host lattice consisting of all other atoms. An approximation is that the embedding energy

depends only on the environment immediately around the impurity or locally uniform electron density. The energy of an impurity atom in a host consists of two terms: the one is a function of the electron density of the host without impurity and the other is the short range electrostatic interaction. The total energy is a sum over all individual contributions of the host and the impurity. Daw and Baskes determined the embedding energies semiempirically and calculated the adsorption energies on the surfaces of Pd and Ni. Agreements with experimental values were fairly good for Pd, but calculated values were much smaller than experiments for Ni. For the bcc iron-hydrogen system, Wen et al. proposed a new potential to be used for the EAM calculation [20]. Using empirically determined parameters for fitting, Wen et al. obtained good agreements between calculated and experimental values for the heat of solution, migration energy, binding energy to vacancies of hydrogen.

On the other hand, the local electronic structure or the bond nature of hydrogen in α-Fe was investigated using a molecular orbital cluster method [21]. The one-electron Hamiltonian for the cluster consists of kinetic energy, Coulomb potential and exchange-correlation interaction potential terms. The last term was expressed in a form proportional to the cubic root of the spin density, and the discrete variational method (DV-Xα) was applied to calculate the elements of the secular matrix equation. Calculations of the density of states for α-Fe clusters of 32 atoms with and without 1 hydrogen atom showed that the main bonding peak was due to H-1s and Fe-4s hybridization with smaller contributions of Fe-3d and 4p. The charge transfer of about 0.6e from the first and second neighbor Fe atoms to H was shown to decrease metallic bond strength. The bond order as a measure of bond strength was calculated as a function of the Fe-H interatomic distance [21]. Interstitial hydrogen notably decreases Fe-Fe bond strength, but acts over a small distance within 0.3 nm. The Fe-H bond strength increases by nearby vacancies associated with a shift of the position of hydrogen atom toward the vacancy.

The total energy of many-electron system at the ground state is determined by using functions of the spatially dependent electron density. The density functional theory (DFT) using a pseudo-potential and a plane-wave basis set was applied by Tateyama et al. to calculate the total energy of H-α-Fe system [22]. A supercell consisting of 54-atoms (53 Fe atoms + 1 H-atom) was adopted locating hydrogen at a T-site as the ground state. The calculated heat of solution was 32.8 kJ/mol-H, which corresponded to an experimentally determined value of 29 kJ/mol-H. Effects of the supercell size or applied pressure on the total energy of the system were also calculated [23]. The calculated heat of solution was a decreasing function of hydrostatic tensile stress that increased cell volume. It is a natural consequence of the repulsive nature of solid solution. It was deduced that the hydrogen concentration in a stress-concentrated region, e.g., ahead of a crack tip, increases about 100-fold by 2–5 GPa of hydrostatic tensile stress.

References

1. Y.G. Huang, K. Fujita, H. Uchida, Bull. Jpn. Inst. Metals **18**, 694–703 (1979)
2. J.R.G. da Silva, S.W. Stafford, R.B. McLellan, J. Less Common Metals **49**, 407–420 (1976)
3. J.P. Hirth, Metall. Trans. A: **11A**, 861–890 (1980)
4. H.P. van Leeuwen, in *Hydrogen Degradation of Ferrous Alloys*, ed. by R.A. Oriani, J.P. Hirth, M. Smialowski (Noyes Pub., Park Ridge, 1985), pp. 16–35
5. G.R. Caskey Jr., in *Hydrogen Degradation of Ferrous Alloys*, ed. by R.A. Oriani, J.P. Hirth, M. Smialowski (Noyes Pub., Park Ridge, 1985), pp. 822–862
6. K. Takai, K. Murakami, N. Yabe, H. Suzuki, Y. Hagiwara, J. Jpn. Inst. Metals **72**, 448–456 (2008)
7. K. Kiuchi, R.B. McLellan, Acta Metall. **31**, 961–984 (1983)
8. Y. Yagi, T. Kobayashi, S. Nakamura, F. Kano, K. Watanabe, Y. Fukai, S. Koike, Phys. Rev. B **33**, 5121–5123 (1986)
9. Y. Yagi, T. Kobayashi, Y. Fukai, K. Watanabe, J. Phys. Soc. Jpn. **52**, 3441–3447 (1983)
10. E. Yagi, ISIJ Int. **43**, 505–513 (2003)
11. C. Sugi, E. Yagi, Y. Okada, S. Koike, T. Sugawara, T. Shishido, K. Ogiwara, J. Phys. Soc. Jpn. **82**, 074601 (2013)
12. H. Wagenblast, H.A. Wriedt, Metall. Trans. **2**, 1393–1397 (1971)
13. J. O'M Bockris, P.K. Subramanyan, Acta Metall. **19**, 1205–1208 (1971)
14. H.A. Wriedt, R.A. Oriani, Acta Metall. **18**, 753–760 (1970)
15. K. Ichitani, M. Kanno, S. Kuramoto, ISIJ Int. **43**, 496–504 (2003)
16. J.K. Nørskov, Phys. Rev. B **26**, 2875–2885 (1982)
17. W.J. Arnoult, R.B. McLellan, Acta Metall. **21**, 1397–1396 (1973)
18. M.S. Daw, M.I. Baskes, Phys. Rev. Lett. **50**, 1285–1288 (1983)
19. M.S. Daw, M.I. Baskes, Phys. Rev. B **29**, 6443–6453 (1984)
20. M. Wen, X.-J. Xu, S. Fukuyama, K. Yokogawa, J. Mater. Res. **16**, 3496–3502 (2001)
21. Y. Itsumi, D.E. Ellis, J. Mater. Res. **11**, 2206–2213 (1996)
22. Y. Tateyama, T. Miyazaki, T. Ohno: Phys. Rev. B, 67, 174105-1-10 (2003)
23. Y. Tateyama, T. Ohno, ISIJ Int. **43**, 573–578 (2003)